You might find this additional information useful...

This article cites 47 articles, 25 of which you can access free at:
http://ajprenal.physiology.org/cgi/content/full/293/5/F1545#BIBL

Updated information and services including high-resolution figures, can be found at:
http://ajprenal.physiology.org/cgi/content/full/293/5/F1545

Additional material and information about *AJP - Renal Physiology* can be found at:
http://www.the-aps.org/publications/ajprenal

This information is current as of November 28, 2007 .

Synchronization among mechanisms of renal autoregulation is reduced in hypertensive rats

Olga V. Sosnovtseva,[1] Alexey N. Pavlov,[2] Erik Mosekilde,[1] Kay-Pong Yip,[3] Niels-Henrik Holstein-Rathlou,[4] and Donald J. Marsh[5]

[1]*Department of Physics, The Technical University of Denmark, Kongens Lyngby, Denmark;* [2]*Department of Physics, Saratov State University, Saratov, Russia;* [3]*Department of Physiology and Biophysics, University of South Florida School of Medicine, Tampa, Florida;* [4]*Department of Medical Physiology, University of Copenhagen, Copenhagen, Denmark; and* [5]*Department of Molecular Pharmacology, Physiology, and Biotechnology, Brown University, Providence, Rhode Island*

Sosnovtseva OV, Pavlov AN, Mosekilde E, Yip K-P, Holstein-Rathlou N-H, Marsh DJ. Synchronization among mechanisms of renal autoregulation is reduced in hypertensive rats. *Am J Physiol Renal Physiol* 293: F1545–F1555, 2007. First published August 29, 2007; doi:10.1152/ajprenal.00054.2007.—We searched for synchronization among autoregulation mechanisms using wavelet transforms applied to tubular pressure recordings in nephron pairs from the surface of rat kidneys. Nephrons have two oscillatory modes in the regulation of their pressures and flows: a faster (100–200 mHz) myogenic mode, and a slower (20–40 mHz) oscillation in tubuloglomerular feedback (TGF). These mechanisms interact; the TGF mode modulates both the amplitude and the frequency of the myogenic mode. Nephrons also communicate with each other using vascular signals triggered by membrane events in arteriolar smooth muscle cells. In addition, the TGF oscillation changes in hypertension to an irregular fluctuation with characteristics of deterministic chaos. The analysis shows that, within single nephrons of normotensive rats, the myogenic mode and TGF are synchronized at discrete frequency ratios, with 5:1 most common. There is no distinct synchronization ratio in spontaneously hypertensive rats (SHR). In normotensive rats, full synchronization of both TGF and myogenic modes is the most probable state for pairs of nephrons originating in a common cortical radial artery. For SHR, full synchronization is less probable; most common in SHR is a state of partial synchronization with entrainment between neighboring nephrons for only one of the modes. Modulation of the myogenic mode by the TGF mode is much stronger in hypertensive than in normotensive rats. Synchronization among nephrons forms the basis for an integrated reaction to blood pressure fluctuations. Reduced synchronization in SHR suggests that the effectiveness of the coordinated response is impaired in hypertension.

tubuloglomerular feedback; myogenic mechanism; oscillations; wavelet analysis

TUBULOGLOMERULAR FEEDBACK (TGF) and the myogenic mechanism combine to provide autoregulation of renal blood flow and limit excursions in glomerular filtration rate (GFR) that fluctuations in arterial pressure (9, 28) might otherwise cause. Both renal mechanisms oscillate autonomously over physiological ranges of blood pressure (11, 21, 22, 53): TGF at 20–40 MHz and the myogenic mechanism at 100–200 MHz (2, 53). The two oscillations interact, with TGF providing modulation of both the amplitude and frequency of the myogenic oscillation (31, 43). In addition, when two nephrons draw

their blood supply from a common cortical radial artery, a change in the activity of TGF in one affects TGF activity in the other (1, 8, 16, 48, 52). The tubular pressure oscillations of two such nephrons appear to synchronize, reflecting the interaction between them. Nephrons from different cortical radial arteries [formerly known as the interlobular artery (17)] appear not to synchronize.

The limit cycle oscillation in TGF arises because of a relatively high feedback gain connected with a number of nonlinearities and delays in the system.[1] Mass epithelial transport of Na and Cl, particularly in the thick ascending limbs of Henle's loop (12, 20), the dependence of the tubular feedback signal on flow rate of tubular fluid, the effect of tubular compliance on fluid wave propagation velocity (38), signal propagation from the macula densa to vascular smooth muscle cells in the afferent arteriole, and the outflow resistance into the distal tubule (12, 27) all contribute to the aggregate delay. We have suggested that the myogenic oscillation arises from nonlinear interactions among voltage and Ca-sensitive K channels and voltage-gated Ca channels in the plasma membrane of vascular smooth muscle cells (29). The TGF and myogenic mechanisms interact because they share a common contractile machinery in vascular smooth muscle cells (29).

Interactions of nonlinear oscillators can give rise to a number of phenomena, such as amplitude and frequency modulation, synchronization, and transitions to chaos. This last phenomenon is of particular interest, because our laboratory has shown that tubular pressure fluctuations in rats with renovascular or genetic hypertension are irregular (10, 52, 54, 55). Power spectra derived from such records show power distributed over a broad frequency band, and the data have characteristics of deterministic chaos (54, 55). Tubular pressure fluctuations from neighboring nephrons of hypertensive rats appear to synchronize (52); synchronization of chaotic systems is also well known (32, 34).

The problem at hand is to test for the presence and the durability of interactions in the systems providing renal blood

---

[1] Nonlinear systems that are second order or higher and that combine an unstable (focus) equilibrium point with dissipative terms can sustain oscillations that return to a stable periodic orbit when perturbed. These periodic orbits are known as limit cycle oscillations. Physiological systems need to respond to perturbations and are invariably dissipative. The transition in which the equilibrium point turns into an unstable focus is a Hopf bifurcation.

Address for reprint requests and other correspondence: D. J. Marsh, Dept. of Molecular Pharmacology, Physiology, and Biotechnology, Brown Univ., Box G-B5, 171 Meeting St., Providence, RI 02912 (e-mail: marsh@ash.biomed.brown.edu).

flow regulation. Previous work on this problem has concentrated on interactions between the TGF and myogenic modes in single nephrons and has made use of whole kidney blood flow measurements (2), tubular pressure measurements from stop-flow (3, 36) and free-flow experiments (41, 43), or single-nephron blood flow (29). We reported previously that the sensitivity of myogenic oscillations to the activity of the TGF mode is much stronger in hypertensive rats (43), a conclusion in agreement with that of Raghavan et al. (36), who analyzed TGF myogenic interactions in stop-flow experiments in single nephrons.

None of these approaches measured synchronization between nephrons, and none analyzed the TGF-myogenic interaction in the context of nephron synchronization, in either normotensive or hypertensive rats. In this study, we present results from the systematic quantitative analysis of free-flow tubular pressure recorded from paired sets of nephrons (52) using wavelet transforms, which are analytic techniques (42) more sophisticated than those available when the experimental recordings were first published. Wavelet analysis enabled us to assess both frequency adjustments and phase synchronization as independent measures of interactions. The nephrons were positively identified as having arisen from single cortical radial arteries and were therefore able to exchange signals because of their vascular proximity (1, 8, 16, 48, 52). The data sets included results from both normotensive and spontaneously hypertensive rats (SHR).

Because each nephron has both TGF and myogenic oscillations, a form of synchronization between neighboring nephrons may occur in which both TGF and the myogenic mechanisms show frequency and phase adjustments and the two nephrons achieve an overall 1:1 synchronization for both the TGF and the myogenic modes, a state we shall refer to as bimodal synchronization. Alternatively, there may be states of partial synchronization, in which some of the rhythmic components synchronize, but others do not. We found bimodal synchronization between nephrons to be typical of normotensive rats and partial synchronization more characteristic of hypertensive rats. The partial synchronization of hypertensive rats can involve either the myogenic oscillations of the neighboring nephrons alone or the TGF oscillations alone. The result with hypertensive rats is counterintuitive, because nephron connection strength is greater in hypertensive than in normotensive rats (1, 5, 23, 48).

The significance of these observations is that synchronization among oscillating units can form the basis of self-organized ensembles that act as a coherent whole. Synchronization at discrete frequencies among neurons in different regions of the brain is now well known as the basis for a good deal of integrated neuronal activity (39). What an ensemble of synchronized nephrons might be able to achieve is not presently known, but it is noteworthy that the synchronization is less complete in hypertension, a disease state in which the ability to excrete Na is known to be problematic.

METHODS

Experimental methods. All experimental results were from work published previously (52). The experiments were performed at the University of Southern California School of Medicine and conformed to then extant policies of the American Physiological Society and of the University of Southern California for use of animals in research. The experimental protocols were reviewed by the Institutional Animal Care and Use Committee of the University of Southern California and were approved by that Committee. No new experiments were performed for this paper. Experiments were performed in male Sprague-Dawley rats, 250–300 g body wt, and in 220–260 g body wt SHR. Anesthesia was induced and maintained with 5% halothane in a gas mixture containing 25% oxygen and 75% nitrogen. Maintenance anesthesia was administered through a tracheotomy tube by means of a respirator, blood pH was maintained between 7.35 and 7.45, and body temperature at 37°C. Simultaneous paired measurements of tubular pressure from two or three surface nephrons of the left kidney were made with the servo-nulling technique for up to 21 min. The 13 normotensive rats had a mean arterial pressure of 111 ± 3 mmHg, and the 18 SHR a mean arterial pressure of 144 ± 5 mmHg. The normotensive rats provided seven pairs of time series from nephrons that were not coupled, and nine pairs of times series from coupled nephrons. The SHR gave 10 pairs of time series from uncoupled nephrons and 11 pairs of time series from coupled nephrons. Vascular coupling here is defined as an origin of both nephrons of the pair from a single cortical radial artery and was confirmed after each experiment by the preparation and examination of silicone casts of the renal vasculature.

Tubular pressure data were recorded through a low-pass Butterworth filter with a cutoff frequency of 1.5 Hz. The data records, which varied in length from 240 to 1,260 s, were then digitized. The rate of digitization was varied, depending on the length of the recording, to produce records with 4,096 points in each of the paired samples. The respiratory signal was removed with a Kaiser-Bessel low-pass filter with a cutoff frequency of 0.5 Hz and attenuation of 50 dB. The calculations reported in this paper were performed on the output of the Kaiser-Bessel filter.

Data analysis. Because of the presence of a number of different modes, the renal tubular pressure signals, like other physiological signals, should be expected to be both inhomogeneous and nonstationary. The results of Raghavan et al. (36) conform to this description. Techniques based on wavelet analysis are widely used to analyze problems of this sort (4, 7, 26, 46, 47). Wavelets provide a tool for detecting periodicities in short, nonstationary data and for following the temporal evolution of different rhythmic components in the case of noisy multimode dynamics.

The wavelet transform (W) of a signal $x(t)$ can be written as:

$$W_x(a,b) = \frac{1}{\sqrt{a}} \int_{-\infty}^{\infty} x(t) \psi_{a,b}^*(t)\, dt \qquad (1)$$

where $\psi(\tau)$ is referred to as the "mother" function; $\psi_{a,b} = \psi[(t - b)/a]$ is a translated and scaled version of this function, with a and b characterizing the time scale and temporal localization, respectively; the asterisk refers to the complex conjugate; and $x(t)$ is the time series. To detect the presence of various rhythmic components, the Morlet-wavelet is particularly useful. The simplified expression of this wavelet has the form:

$$\psi(\tau) = \pi^{-1/4} \exp(j2\pi f_0 \tau) \exp\left(-\frac{\tau^2}{2}\right) \qquad (2)$$

The Morlet wavelet represents a harmonic function modulated in amplitude by a Gaussian. The parameter f_0 defines an observation window and determines the number of oscillations of the wavelet within it. For the purpose of this work, we can use $f_0 = 1$. Increasing f_0 improves frequency resolution but reduces temporal resolution. The relation between the scale a and the central frequency f for the scaled function is $f = 1/a$. The mean value of each time series was subtracted from each term before the wavelet transform was applied.

In addition to the wavelet transform coefficients $W_x(a,b)$ [or $W_x(f,b)$], the power spectral density $E_x(f,b) \sim |W_x(f,b)|^2$ can be estimated. The result is a surface in three-dimensional space $E_x(f,b)$ whose sections at fixed time moments $b = t_0$ correspond to the local

power spectrum. To simplify the visualization of this surface, only the dynamics of the local maxima of $E_x(f,b)$, the time evolution of the spectral peaks, are estimated (15). This approach allows us to extract the time dependencies of the instantaneous frequencies for the rhythmic components of the signal.

For the analysis of the temporal variation of the proximal tubular pressure in adjacent nephrons, one can distinguish four potential states of their interactive dynamics: *1*) bimodal coherence when the instantaneous frequencies for both oscillatory modes remain close in time; *2*) the completely incoherent state; and *3*) the two states of partial entrainment where coherence is observed for only one of the oscillatory modes. An approach based directly on the frequency adjustment is simple and has a clear physical interpretation, but it cannot detect a phase shift between the oscillations of the two interacting nephrons.

Tubular pressure in SHR fluctuates irregularly and generates power spectra with many different peaks (52, 54). Because we apply wavelet transforms to such records in this study, it will be useful to describe some of the special problems that might arise and how we deal with them. The instantaneous frequency of TGF can change its value in time in SHR more than is usually found in normotensive rats. The standard power spectrum provides an average value for each frequency over the entire observation period; a single process that changes its frequency over the course of the observation can generate more than a single spectral peak, even though it has just one instantaneous frequency at each moment in time. The single process is easily identified with the wavelet transform, despite its variation in time. Thus the presence of spectral peaks in adjacent frequency bands in SHR does not imply that there are fluctuations at two frequencies at the same time.

Second harmonics of the TGF oscillation are easily identified in the wavelet transform process because they have a frequency twice that of the TGF fluctuation (higher order harmonics usually have negligible power), and synchronization of harmonics was not included in our analysis.

Phase synchronization provides an alternative measure of entrainment phenomena in interacting systems (34, 37). In an earlier paper (13), we studied phase relations between two signals using a Hilbert transform. This approach works well when the signal has a dominant rhythmic component, but not with the separate dynamics of different rhythmic activities. In this study, the multimode process has one clearly expressed rhythm, the slow TGF oscillation, whereas the signature of the myogenic rhythm in the proximal tubular pressure records is much weaker. A separate investigation of the two modes could perhaps be accomplished after band-pass filtering to extract the frequency ranges associated with each mode. However, the filtering process can cause many technical problems in the case of nonstationary dynamics, especially if the two modes are closely positioned in the frequency domain and in the presence of significant harmonics and combination frequencies. Problems of this type can sometimes be solved by using a sliding window analysis (45), but the case in which the modes synchronize remains intractable with this technique. The wavelet approach represents the most effective way to study the different aspects of multimode phase dynamics. Instantaneous phases can be introduced via the wavelet-transform coefficients as follows:

$$W_x(f,b) = |W_x(f,b)| \cdot \exp[i\varphi_x(f,b)] \qquad (3)$$

where the phase function $\varphi_x(f,b)$ depends on the mode being analyzed. Lachaux et al. (18) and Quiroga et al. (35) used the definition of phase in *Eq. 3* to analyze synchronization properties in EEG signals. They studied phase relations over a range of values of f by fixing the frequency and considering how the phase differences change with b.

In general, the wavelet transform provides us with two-dimensional arrays of moduli $W_x(f,b)$ and phase $\varphi_x(f,b)$. This means that the notion of phase is defined for each frequency f at any fixed time moment b. When considering two processes $x(t)$ and $y(t)$, the wavelet transform allows us to calculate the phase differences $\varphi_x(f,b) - \varphi_y(f,b)$ and various synchronization factors (35). In the case of clearly expressed multimode dynamics, we do not need to know the complete

two-dimensional phase spectrum $\varphi_x(f,b)$, because we are interested only in phases related to the characteristic rhythmic contributions. If the instantaneous frequencies demonstrate large fluctuations relative to the mean value, it is useful to adjust the central frequency of the wavelet function according to these fluctuations. Hence we will modify slightly the approach considered in Refs. 18 and 35. We follow the time evolution of each mode in the frequency domain, and, at fixed moments of time $b = t_0$, we extract the phases related to the local peaks of the power spectrum $E_x(f,t_0)$. For coupled nephrons, this permits introduction of the phase for the slow and the fast dynamics separately.

For two interacting self-sustained systems, synchronization manifests itself as an adjustment of their basic frequencies to satisfy the relation $nf_1 = mf_2$. In our analysis, we have restricted the values of the integers m and n to 10 or less, so as to consider only simple resonances. Another manifestation of synchronization is a phase adjustment in the interacting systems. The condition of phase synchronization may be expressed as:

$$|n\varphi_1 - m\varphi_2 - C| < \gamma \qquad (4)$$

where $n\varphi_1 - m\varphi_2 = \Delta\varphi$ is the relative phase difference; φ_k, $k = 1,2$ are phases of *signals 1* and *2*; $\gamma < 2\pi$ is the limit used to define synchronization, as discussed below; and C is a constant whose value is chosen so that $\Delta\varphi = 0$ at $t = 0$. All subsequent estimated values of $\Delta\varphi$ are relative to that initial value. If interacting systems are periodic and subject to noise, chaotic, or both, *Eq. 4* may only remain satisfied during a finite time interval (44). In this case, a regime is considered to be synchronous when the duration of the locking time, the region over which *Eq. 4* is satisfied, exceeds some predefined number of basic oscillatory periods (25). We took the predefined number to be the duration of eight periods of a particular oscillation, which translates to 250 s for the slow oscillations and 50 s for the fast.

Results are presented as means ± 1 SE. Statistical significance was estimated using the Mann-Whitney test.

RESULTS

Time frequency resolution of the wavelet method. Figure 1 illustrates the ability of the wavelet approach to detect and follow changes in the instantaneous frequency of a signal. Each part has two panels. The *top* panel displays the test signal to be analyzed, and the *bottom* panel shows the detected frequency (or frequencies). The *top* panel of Fig. 1*A* shows a nonstationary time series used by Chon et al. (3) to illustrate the ability of a time frequency spectral method to extract different frequencies. The *bottom* panel shows the frequencies calculated with our wavelet method. The result is exactly the same as reported by Chon et al. During the first 200 s, we detect a frequency of 0.02 Hz. During the following 100 s, no detection is made, as the amplitude of the signal vanishes, and, for the last 200 s, we detect a signal of 0.1 Hz. The *top* panel of Fig. 1*B* shows a time series in which the frequency of oscillation is switched from 0.01 to 0.03 Hz. The *bottom* panel of Fig. 1*B* shows the result obtained with wavelet transforms. The change in frequencies is detected and over a time interval less than one cycle of the higher frequency. The *top* panel of Fig. 1*C* shows a time series resulting from the addition of two signals with linearly increasing frequencies. The result, shown in the *bottom* panel, is the same as reported by Wang et al. (50), although they extended the time series to higher frequencies. The *top* panel of Fig. 1*D* shows a time series that begins at the lowest TGF frequency we observed in SHR and that increases linearly with time to double within a single period of the initial cycle. The results obtained with wavelet transforms show that
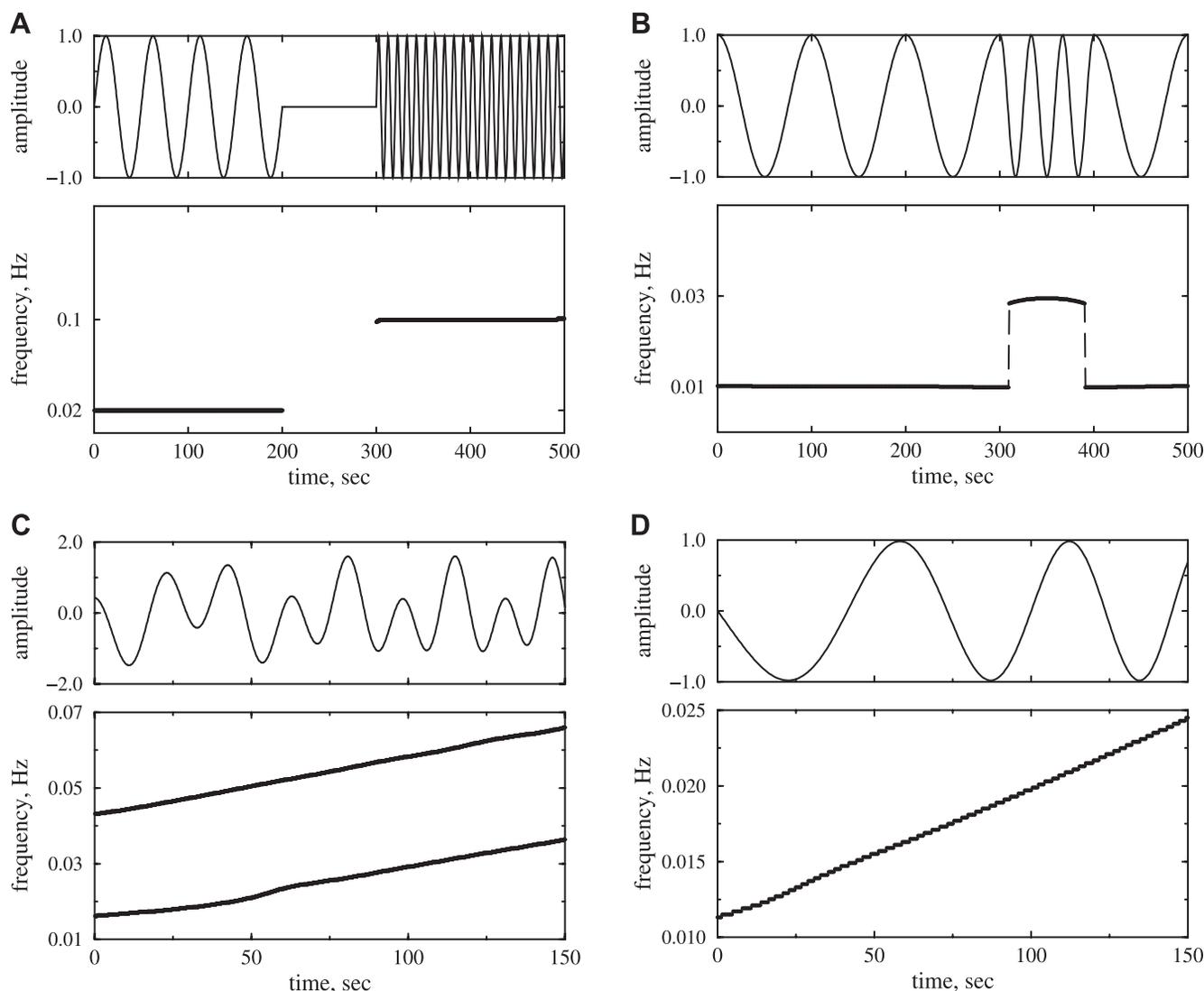
Fig. 1. *A*, *top*: nonstationary time series with two frequencies, each appearing over different time intervals. *Bottom*: frequency vs. time, determined with wavelet transforms. *B*, *top*: nonstationary time series switching between 0.01 and 0.03 Hz. *Bottom*: frequency vs. time estimated with wavelet transforms. *C*, *top*: two superimposed signals, each with increasing frequency, at frequencies characteristic of tubuloglomerular feedback (TGF) and the myogenic mechanism. *Bottom*: frequency vs. time, determined with wavelet transforms. *D*, *top*: nonstationary time series beginning at 0.01 Hz, the lowest frequency observed in SHR recordings and doubling in frequency within a single cycle. *Bottom*: wavelet transform.

the method accurately detects the frequency change. These results show that wavelet methods provide frequency resolution comparable to time frequency spectral methods, a comparison that is well supported in the literature (4, 6, 26), and that they satisfy the frequency requirements of the data sets to which we have applied them.

Bimodal oscillations in nephron autoregulation. Averaged power spectra for 32 time series from normotensive rats are in Fig. 2*A*, and 42 time series from SHR are in Fig. 2*B*. The tubular pressure time series we analyzed varied in length from 240 to 1,260 s and were sampled at rates designed to produce time series of 4,096 points. The spectrum from normotensive rats shows a sharp peak at a frequency of ~0.03 Hz, corresponding to the slow TGF-mediated oscillations and a wider peak from the myogenic mechanism in the range 0.10–0.20 Hz. The same peaks can be detected in the data from hypertensive rats, although they are significantly smaller and broader, reflecting the irregularity of the signal. These results

were obtained by calculating single power spectra from each experimental time series and averaging all of the power spectra in each group of animals, a method that provides no temporal resolution.

Distribution histograms from the results of wavelet analysis applied to the individual time series are shown in Fig. 3. The analysis resolves each of the power spectra shown in Fig. 2, *A* and *B*, into the underlying two modes. Each data set is unimodal and approximately normally distributed, justifying the use of a single mean and SE to characterize each of the data sets, as is done in Table 1. The figure confirms that the slow oscillation in normotensive rats is more constrained over the frequency range than in SHR.

Results of statistical analysis from wavelet analysis over all recordings are in Table 1. To obtain these results, wavelet analysis was applied to each time series to obtain the instantaneous amplitude and frequency for the two mechanisms. Averages of the instantaneous values from each time series
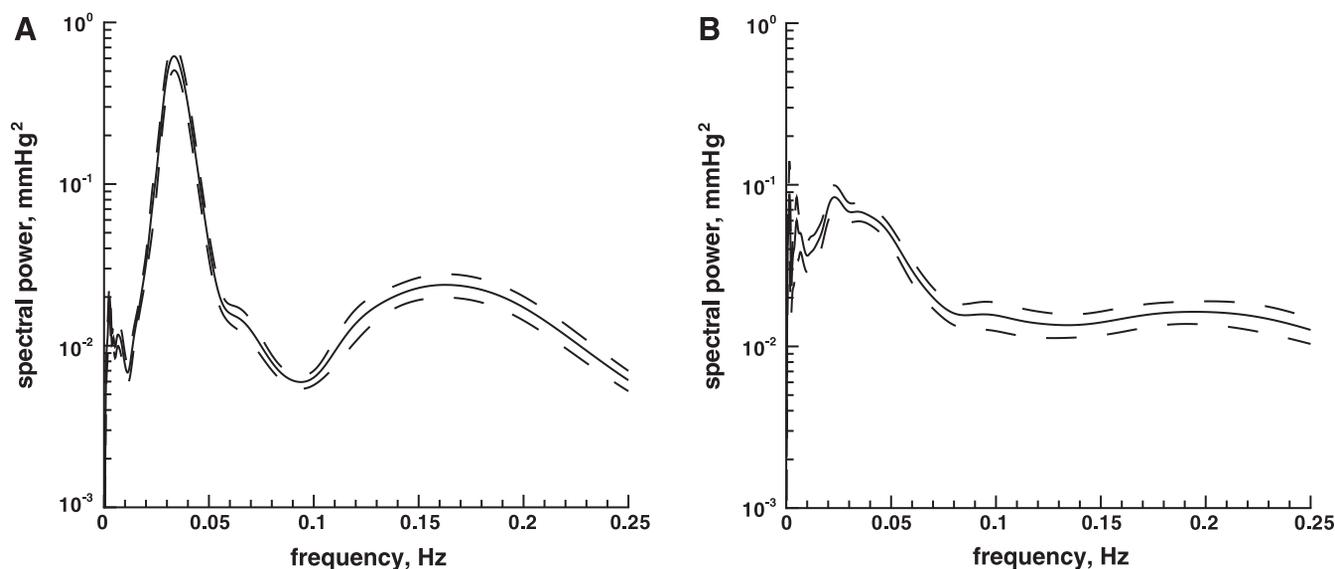
Fig. 2. Averaged power spectra of tubular pressure variations for 32 time series from normotensive rats (*A*) and 42 time series from spontaneously hypertensive rats (SHR; *B*). Values are shown as means $\pm$ 1 SE.

were obtained and used to derive the population averages in the table. Each of the distributions whose average values are given in Table 1 was approximately normal, as can be seen in Fig. 3. Although the results in Fig. 2 suggest greater variability in the frequencies of both TGF and the myogenic oscillations in SHR, application of two-dimensional wavelets permits us to extract both oscillations from each time series and to analyze the entrainment phenomena.

Interactions between TGF and myogenic oscillations in single nephrons. We first consider the case of intranephron interaction of the two modes. Figure 4 shows distributions of the ratio $f_{fast}(t)/f_{slow}(t)$, where $f_{slow}(t)$ and $f_{fast}(t)$ are the frequencies of the TGF-mediated and the myogenic oscillations, respectively. The distribution obtained for normotensive rats, shown in Fig. 4*A*, has two peaks corresponding to the ratios 4 and 5. This implies that the fast and the slow components adjust their periods in such a way as to maintain a near 4:1 or 5:1 entrainment during significant parts of the observation time. The shoulder on the left-hand side of the 5:1 indicates the presence of intervals with 6:1 synchronization. For the chaotic oscillations observed for the hypertensive rats, shown in Fig. 4*B*, the frequency ratio changes more randomly in time. There is only a single broad peak in the probability density, and the nephron dynamics show mutual adjustments only for time intervals that are too short to be clearly expressed in the averaged distribution of the ratio $f_{fast}(t)/f_{slow}(t)$. Examples illustrating how this ratio changes in time were presented by Sosnovtseva et al. (42).

The self-sustained pressure fluctuations due to TGF can be periodic or chaotic in each nephron, and the same is necessarily true for the myogenic oscillations. The fluctuations from each mechanism can be synchronous or asynchronous with respect to each other in a single nephron. As we shall see, these variations play a role in the synchronization between interacting nephrons.

Synchronization of interacting nephrons. Vascular casts were used to test whether pairs of superficial nephrons used for tubular pressure measurements had afferent arterioles branch-

ing from a single cortical radial artery (52). We shall refer to those pairs that had origins from the same cortical radial artery as neighboring nephrons. Figure 5 illustrates two different synchronization states that can occur in a pair of neighboring nephrons. In Fig. 5*A*, the ratio $f_1(t)/f_2(t)$ between the frequencies in the two nephrons remain close to 1:1 throughout the observed time interval for both the slow and the fast modes. One can observe some fluctuation in the frequency ratio, particularly for the fast modes, but the amplitude of this fluctuation remains within a limit of $\pm 10\%$ of the nominal frequency. In Fig. 5*B*, on the other hand, the only synchronization between the two nephrons is in the slow mode. The frequency ratio of the fast mode varies over the time course of the experiment, exceeding the 10% limit for more than one-half the observation time and does not settle at a plateau at or near 1.00. Figure 5*B* illustrates a case of partial synchronization.

For each pair of experimental data series, we determined the time intervals where the modulus of the difference between the corresponding instantaneous frequencies did not exceed a predetermined fixed value. The oscillations are synchronous in these intervals. We have chosen the limits of the synchronous dynamics to be $\pm 10\%$ of the value of the mean instantaneous frequency: ± 0.003 Hz for the slow mode and ± 0.015 Hz for the fast mode. Other limits produce similar results, except that a widening of the limits results in longer locking times; the qualitative picture, and in particular the distinctions between two rat strains, remains the same.

As shown in Table 2, there is a difference in synchronization phenomena between the normotensive and the hypertensive rats. Nephrons of normotensive rats supplied from the same cortical radial artery are fully coherent 81% of the time, where both the slow and the fast oscillations synchronize, as seen in Fig. 5*A*. The other combinations of possible dynamics have a significantly lower probability of occurrence. In contrast, the most probable state for the hypertensive rats is one of partial synchronization, where either the slow or the fast rhythms are locked while the other mode remains nonsynchronous, as seen
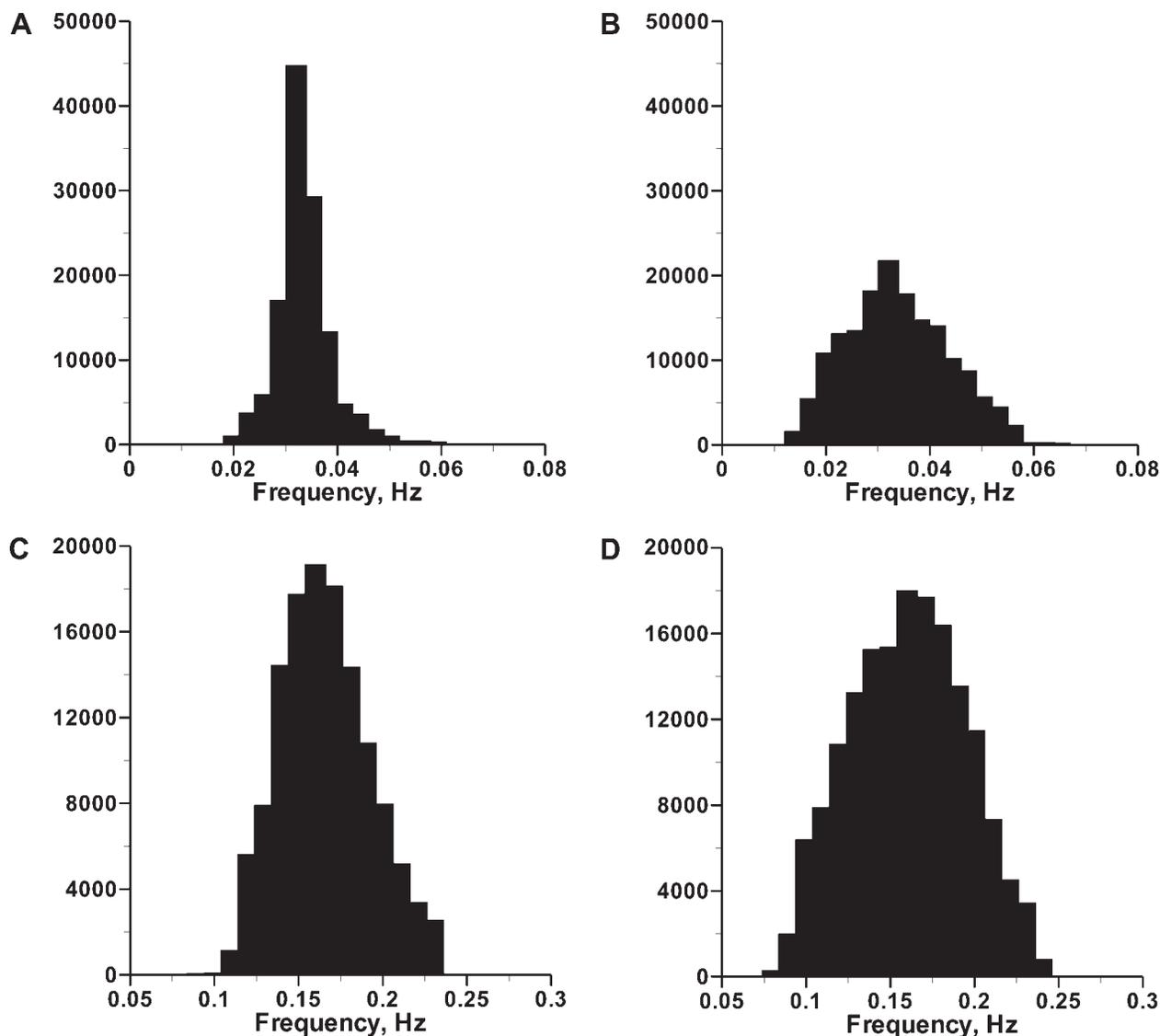
Fig. 3. Distribution histograms from wavelet transforms applied to the individual time series. *A*: low-frequency mode from normotensive rats. *B*: low-frequency mode from SHR. *C*: high-frequency mode from normal rats. *D*: high-frequency mode from SHR. Values of the mean and SE from each of the 4 data sets are in Table 1.

in Fig. 5*B*. The slow mode locks more frequently than the fast mode.

Figure 6 shows the probability of finding different time intervals of coherent dynamics. In normotensive rats, the slow TGF-mediated oscillations have a probability of 40% of remaining synchronized longer than 250 s, a duration that represents eight or more periods of the oscillation. For hypertensive rats, that probability is only 12%. Fast myogenic oscil-

lations similarly have a probability of ~30% of remaining synchronized for more than 50 s, corresponding to eight periods of the myogenic oscillations, while for hypertensive rats this probability is only 12%. Slow oscillations in normotensive rats are three to four times as likely to display long locking times as in SHR, and a similar factor applies to the fast oscillations.

The mean locking times, under the condition that effective synchronization is defined as a frequency change less than

Table 1. *Mean values of amplitudes and frequencies for the tubuloglomerular feedback and the myogenic modes with the standard errors of the mean obtained from wavelet analysis*

Rats	Slow Mode		Fast Mode	
	Amplitude, mmHg	Frequency, Hz	Amplitude, mmHg	Frequency, Hz
Normotensive	0.80 ± 0.08	0.033 ± 0.001	0.17 ± 0.012	0.167 ± 0.005
Hypertensive	0.34 ± 0.021	0.032 ± 0.002	0.13 ± 0.010	0.164 ± 0.006

The 32 recordings from normotensive animals generated 128,796 data points for each of the two modes, and the 42 recordings from spontaneously hypertensive rats gave 164,814 data points.
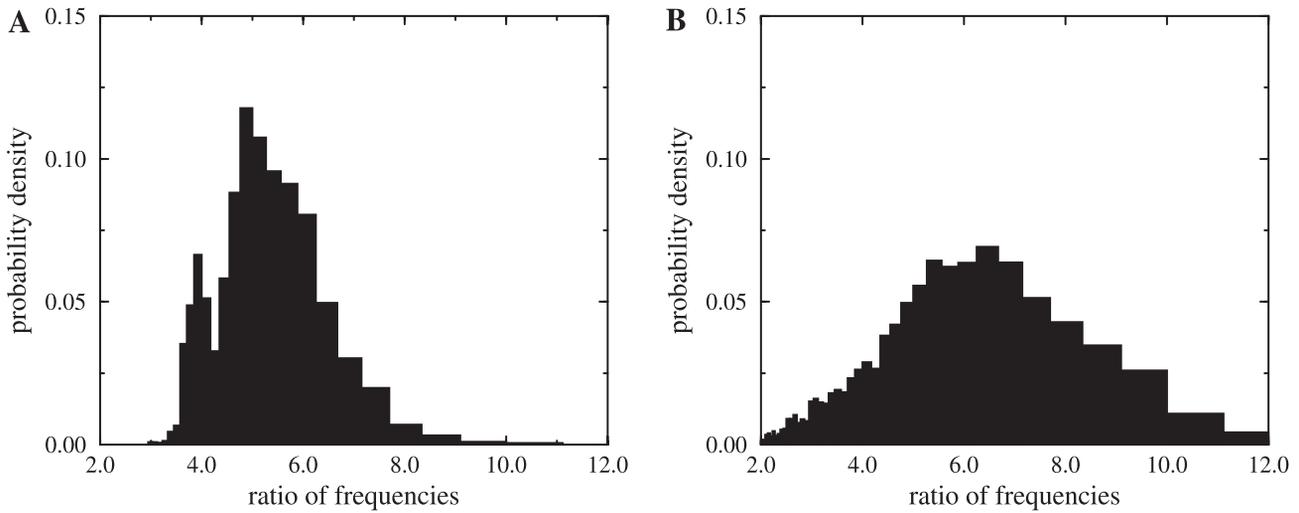
Fig. 4. Distribution of the ratio of the instantaneous frequencies $f_{fast}(t)/f_{slow}(t)$ from 32 time series in normotensive rats (*A*) and 42 time series in SHR (*B*), where $f_{slow}(t)$ and $f_{fast}(t)$ are the frequencies of the TGF-mediated and the myogenic oscillations, respectively.

±10% of the mean instantaneous frequency, were 360 ± 31 s and 75 ± 14 s for the slow and the fast dynamics in normotensive rats; the corresponding locking times for SHR were 100 ± 16 s and 25 ± 4 s, respectively. The differences between normotensive rats and SHR were highly significant for both the slow mode ($P = 0.00003$) and the fast mode ($P = 0.00015$). We conclude that the hypertensive rats demonstrate significantly shorter intervals of coherent dynamics than normotensives.

We also analyzed data from paired nephrons that were found to originate from different cortical radial arteries. In these measurements, we expected to find no interaction because of the origin from different cortical radial arteries, and visual inspection of the original data confirms this expectation (52). For normotensives, the slow oscillation had a mean locking time of 48 ± 5 s and the fast oscillation 27 ± 4 s; for hypertensives, the corresponding findings were 42 ± 6 s and 15 ± 2 s. The estimated locking time of these TGF oscillations is less than two full periods. The results confirm the prediction and also the specificity of the analytic methods.

Phase entrainment of interacting nephrons. Frequency and phase synchronization are useful alternate approaches to evaluating entrainment phenomena in coupled systems (34, 37). The two approaches are not identical, because frequency synchronization characterizes the average behavior of a system over some time interval, while phase synchronization describes the system at each time moment and provides additional information on phase shifts. For chaotic and stochastic systems, these two approaches can give different results. As in the case of frequency adjustments, we need to formulate the conditions under which the dynamics can be considered as synchronous. For 1:1 synchronization, this condition should ensure that the modulus of the phase difference between the oscillations in the paired nephrons does not exceed some fixed value γ. Here, we have chosen $\gamma = 2\pi/10$ for the slow rhythm and $\gamma = 2\pi/6$ for the fast mode. The time series we analyzed are neither stationary nor free of noise, and these factors can cause some variability in the phase-angle difference. The values of γ we chose allow for some variability from these sources. The different values of γ account for a significantly
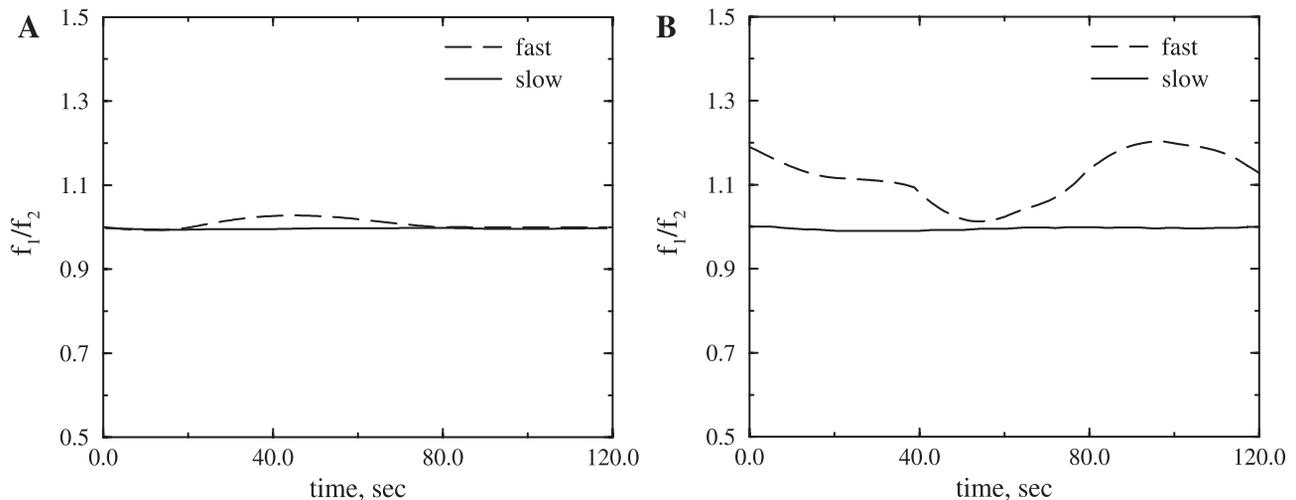

Fig. 5. Bimodal (*A*) and partial (*B*) coherence in the dynamics of paired nephrons for a normotensive and a hypertensive rat, respectively. f_1/f_2, Ratio between the frequencies in the two nephrons.

Table 2. *Probability of different combinations of frequency entrainment in tubular pressure measurements from 9 pairs of nephrons in normotensive rats and 11 pairs of nephrons from hypertensive rats*

	Probability, %	
Type of Dynamics	Normotensive Rats	Hypertensive Rats
Bimodal coherence	81	39
Complete incoherence	0.4	16
Partial coherence		
Only for slow rhythms	13	36
Only for fast rhythms	6	10

higher variability of the myogenic oscillations. The duration of the mean locking time, our measure of the degree of synchronization, depends on the condition applied to the parameter γ, but, even with different conditions for γ, the qualitative synchronous patterns remain the same.

Figure 7*A* shows variations of the normalized phase difference for the regular pressure dynamics in a normotensive rat; the synchronization of the slow and the fast oscillations for nephrons branching from the same cortical radial artery is apparent. Nephron dynamics of a hypertensive rat, shown in Fig. 7*B*, are more complicated, especially with respect to entrainment of the myogenic components. It is possible to find examples where the fast modes demonstrate segments of phase-locked oscillations, although a more typical case is when the phase-locked regime occurs only for short time intervals. Figure 7*B* illustrates partial entrainment because only the slow mode demonstrates intervals of phase-locked dynamics for a longer duration than a single period of the slow oscillations, which is ~30 s.

Table 3 shows the probabilities of finding different states of phase-synchronized dynamics. The results are similar to those obtained with the frequency locking approach. The values given in Tables 2 and 3 can vary, depending on the restrictions used for defining the synchronous state, but they illustrate that paired nephrons in normotensive rats typically show full synchronization where all oscillatory modes are synchronized;

nephrons in hypertensive rats often demonstrate partial entrainment. The total probability of observing partial synchronization, 41%, exceeds the probability of the full synchronization, 35%, and both types of partial synchronization are prominent.

Distinctions in the appearance of large intervals of phase-synchronized dynamics are very similar to those presented in Fig. 6, confirming differences between normotensive and the hypertensive rats. The mean times of phase locking were 270 ± 23 and 60 ± 12 s for the slow and the fast oscillations in normotensive rats, and 90 ± 14 and 20 ± 3 s, respectively, for SHR. The differences between normotensive rats and SHR were highly significant for both the slow mode ($P = 0.000001$) and the fast mode ($P = 0.0014$). Although these results are not exactly the same as those found for frequency entrainment, the relationships among them are similar and support the conclusion that the hypertensive rats have a shorter duration of synchronous dynamics and a higher probability of partial synchronization than their normotensive counterparts.

DISCUSSION

We applied wavelet analysis to experimental data from normotensive and hypertensive rats to evaluate the intra- and internephron interactions of the two oscillatory modes present in kidney autoregulation. These are the fast oscillations associated with myogenic dynamics of the afferent arteriole and the slower oscillations arising from the operation of TGF. We found that the fast and the slow components of nephron dynamics in the normotensive rats maintain a near 4:1 or 5:1 entrainment, although 6:1 entrainment may also occur. Outcomes of the interaction between TGF and the myogenic mechanism include frequency and amplitude modulation (31, 43). The corresponding entrainment phenomena for the SHR are less clearly expressed and occur only for shorter time intervals.

Chon et al. (2) used Volterra-Wiener kernels to estimate interactions between TGF and the myogenic mechanism in whole kidney blood flow records with arterial pressure subject to white noise forcing. They detected nonlinear interactions in normotensive animals, but not in hypertensives. Using bispectrum analysis of tubular pressure measurements from stop-flow
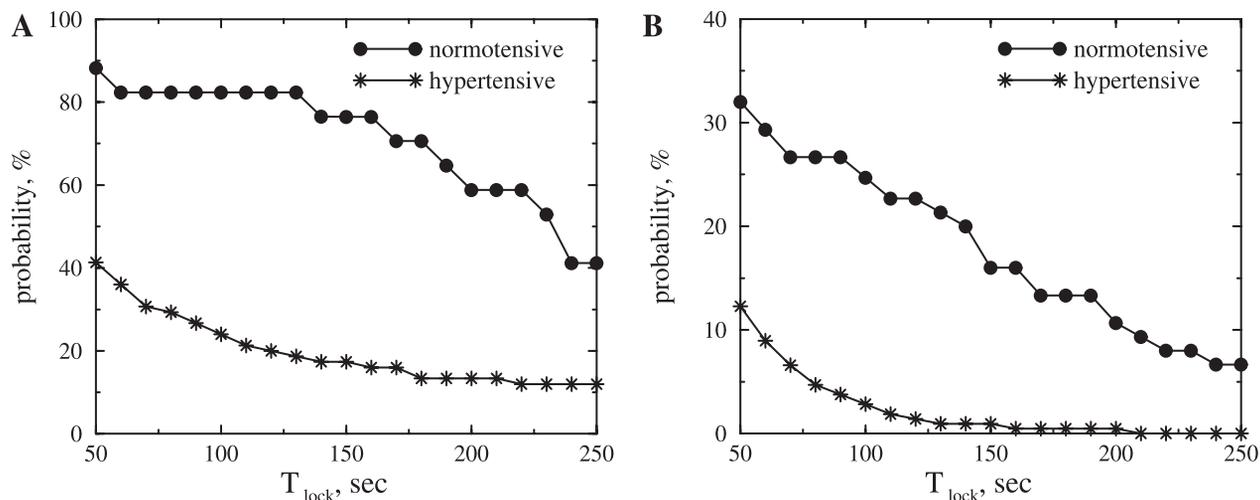

Fig. 6. Probability of finding intervals of frequency locking that exceed locking time (T_{lock}) for the slow (*A*) and the fast (*B*) dynamics. This probability was estimated by calculating the relative number of time series that contain locking intervals larger than T_{lock}. Two data records from normotensive rats and one SHR that were shorter than 600 s were not analyzed for this figure.
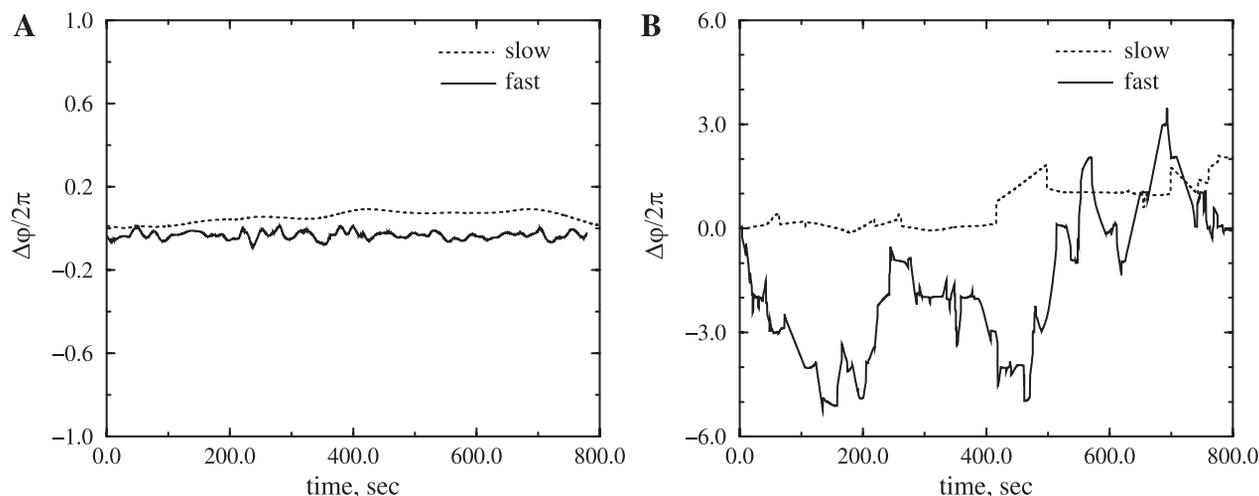
Fig. 7. Phase differences ($\Delta\varphi$) for the slow and the fast oscillations of paired nephrons obtained from a normotensive (*A*) and a hypertensive (*B*) rat. Note the different vertical axes used in *A* and *B*.

experiments, Chon et al. subsequently confirmed the presence of nonlinear interactions between TGF and the myogenic mechanism in normotensive but not in hypertensive animals (3). They speculated that the failure to detect interactions in hypertensives was a defect of the time-invariant bispectral technique. They, therefore, developed a time-varying bispectrum approach and used it to show that nonlinear interactions between TGF and the myogenic mechanism did occur in hypertensive animals, but that the interactions were shorter lived than in normotensives (36). Our analysis of the interaction between the myogenic and TGF modes from free-flow tubular pressure recordings confirms these earlier results, despite the different experimental settings from which the data were collected.

We evaluated synchronization phenomena in interacting nephrons by measuring both frequency and phase synchronization. Statistical analyses performed with these two techniques showed that completely nonsynchronous dynamics are atypical for nephrons of normotensive rats supplied by a common cortical radial artery; the probability of this state ranges from 1 to 5%, depending on whether frequency or phase is assessed. The completely nonsynchronous regime occurs more frequently in the dynamics of the SHR (15–24%). Normotensive rats demonstrate full entrainment in which both oscillatory modes are synchronized; the probability in both tests exceeds 70%. SHR demonstrate a different type of internephron dynamics: partial entrainment where neighboring nephrons attain a state of synchronization with respect to their slow dynamics, but the fast dynamics remain desynchronized,

Table 3. *Probability of different states of phase synchronization in paired nephrons*

	Probability, %	
Type of Dynamics	Normotensive Rats	Hypertensive Rats
Bimodal synchronization	71	35
Nonsynchronous	5	24
Partial synchronization		
Only for slow rhythms	17	28
Only for fast rhythms	7	13

or vice versa. The aggregate probability of partial entrainment exceeds 40% in SHR. SHR generally are in a synchronous state for only one-third to one-half as long as the normotensive ones; they have about one-half the probability of full synchronization and about twice the probability of partial synchronization.

The physiological mechanisms responsible for the various synchronization phenomena we have characterized are largely unknown. We have suggested that the coupling of TGF to the myogenic mechanism takes place in vascular smooth muscle cells and makes use of voltage-gated Ca channels (29), but other coupling routes are possible. Coupling via plasma membrane Ca channels leads to the prediction that the TGF oscillation modulates both the amplitude and the frequency of the myogenic oscillation; analyses of single nephron blood flow data and the results of this study confirm the prediction (31). The modulation of the myogenic mechanism by TGF has been observed in the isolated, perfused juxtamedullary preparation (49). There is also accumulating evidence that nitric oxide modulates the TGF-myogenic interaction (14, 15, 40, 51).

The conduction mechanism for nephron-to-nephron signaling has been subject to very little investigation. Recent work by Peti-Peterdi (33) suggests that a propagated Ca wave is too slow to account for signal conduction, leaving electrotonic conduction as the most likely explanation.

Oscillations such as those we analyzed arise naturally from the operation of nonlinear systems. The interaction of such self-sustained systems can lead to different nonlinear outcomes, including synchronization, amplitude and frequency modulation, and chaos (32). Whether interacting nonlinear oscillators achieve synchronization is a question that arises in many areas of science (32, 34); its functional meaning in renal physiology remains to be discovered. Synchronization of self-sustaining oscillations can permit the ensemble of synchronized units, in this case nephrons, to react in a coordinated fashion to perturbations of the system. Such self-organized systems can take on emergent properties, and, in living systems capable of adaptation, it is natural to assume that the oscillations are system responses designed specifically to generate the emergent functional properties. We suggest that nephron synchronization provides the basis for self-organized action in response to

naturally occurring fluctuations in blood pressure (9). Below we discuss one possible aspect of self-organization in the kidney.

Tubular pressure recordings from rats with hypertension show characteristics of deterministic chaos (54, 55). These characteristics include a positive Lyapunov exponent indicating high sensitivity to initial conditions, a hallmark of chaotic systems, and a low-dimension noninteger phase space attractor (54). The data also pass a test known as surrogate data analysis (55). The test is designed to determine whether noise is responsible for the irregular fluctuations in the signal; when applied to renal tubular pressure records, the test result showed little indication of noise as a factor. Bifurcations to chaos in model systems can occur in a single nonlinear system when the value of the parameter is made to exceed a critical value, or when the coupling strength of an ensemble of nonlinear systems is increased above a critical value. The measured value of TGF gain is almost twice normal in SHR (5, 10), and the coupling strength of nephron-nephron interactions is increased threefold (1, 48). Thus the conditions required for a bifurcation to chaos are present in SHR, and we (30) and Layton et al. (19) have shown in different simulations that the connection strength of internephron coupling can serve as a bifurcation parameter. Although chaotic systems are known to synchronize (32, 34), it is also true that the synchronization is more easily disrupted than when the same nonlinear systems are oscillating (24). From these considerations, we speculate that the increase in the strength of both intra- and internephron coupling is the initial event in the partial disruption of nephron synchronization we observed. It remains to be determined what adaptive purpose, if any, is served by the increase in connection strengths and the bifurcation to chaos in hypertension.

We suggest that the less frequent synchronization we found in SHR could have at least two sets of functional consequences. First, consider the effects on blood flow distribution. We recently simulated the interactions among oscillating nephrons of different lengths supplied by a single cortical radial artery that could be synchronized by vascular signals (30). With no vascular coupling, the simulation showed that the fraction of cortical radial artery blood flow received by each nephron varied with time because the oscillations were not synchronized. Vascular coupling produced synchronization of nephrons and an oscillation of mean vascular pressure in the cortical radial artery, and the fractional delivery of blood to each nephron remained constant throughout the TGF cycle. The results of this study suggest that, because of decreased synchronization, fractional blood flow distribution among nephrons of SHR will be more highly variable, an effect that could cause more highly variable GFR. Episodes of elevated GFR from this source could contribute to impaired regulation of solute excretion and to glomerular damage.

A second consequence of imperfect synchronization among nephrons will likely be irregular delivery of tubular fluid to distal nephron segments. We have found oscillations in distal tubule pressure and of distal tubule Cl concentration at the TGF frequency (11), indicating that fluid delivery to distal segments retains some of the dynamic properties of nephron blood flow and GFR. Cortical collecting tubules and inner medullary collecting ducts receive tubular fluid from a number of nephrons. It is likely that the dynamics of fluid delivery to these tubular junctions will depend on the dynamics of blood flow and GFR

regulation; if nephron blood flows are synchronized, so too will be distal delivery. Noncoherent blood flow regulation among nephrons is likely to cause noncoherent delivery into collecting tubules and ducts. At stake here are flow-dependent K secretion and hormone-dependent reabsorption of Na, Cl, and other ions. Modern understanding of these processes is described only as if the flows remain steady in time. The steady-state formulation is equivalent to an assumption that flow rates in all distal tubules feeding a cortical collecting duct are synchronized. In the absence of synchronization, or if synchronization is intermittent, flow and solute load-dependent processes may not generate time average values equivalent to tubules operating in a steady state. It remains to be seen whether these effects, if they do occur, have functional consequences.

REFERENCES

1. **Chen YM, Yip KP, Marsh DJ, Holstein-Rathlou NH.** Magnitude of TGF-initiated nephron-nephron interactions is increased in SHR. *Am J Physiol Renal Fluid Electrolyte Physiol* 269: F198–F204, 1995.
2. **Chon KH, Chen YM, Marmarelis VZ, Marsh DJ, Holstein-Rathlou NH.** Detection of interactions between myogenic and TGF mechanisms using nonlinear analysis. *Am J Physiol Renal Fluid Electrolyte Physiol* 267: F160–F173, 1994.
3. **Chon KH, Raghavan R, Chen YM, Marsh DJ, Yip KP.** Interactions of TGF-dependent and myogenic oscillations in tubular pressure. *Am J Physiol Renal Physiol* 288: F298–F307, 2005.
4. **Daubechies I.** *Ten Lectures on Wavelets*. Philadelphia, PA: Society for Industrial and Applied Mathematics, 1992.
5. **Dilley JR, Arendshorst WJ.** Enhanced tubuloglomerular feedback activity in rats developing spontaneous hypertension. *Am J Physiol Renal Fluid Electrolyte Physiol* 247: F672–F679, 1984.
6. **Flandrin P.** Some aspects of non-stationary signal processing with emphasis on time-frequency and time-scale methods. In: *Wavelets*, edited by Combes JM, Grossman A, and Tchamitchian PH. Berlin: Springer-Verlag, 1989, p. 68–98.
7. **Grossman A, Morlet J.** Decomposition of Hardy functions into square integrable wavelets of constant shape. *SIAM J Math Analysis* 15: 723–736, 1984.
8. **Holstein-Rathlou NH.** Synchronization of proximal intratubular pressure oscillations: evidence for interaction between nephrons. *Pflügers Arch* 408: 438–443, 1987.
9. **Holstein-Rathlou NH, He J, Wagner AJ, Marsh DJ.** Patterns of blood pressure variability in normotensive and hypertensive rats. *Am J Physiol Regul Integr Comp Physiol* 269: R1230–R1239, 1995.
10. **Holstein-Rathlou NH, Leyssac PP.** TGF-mediated oscillations in the proximal intratubular pressure: differences between spontaneously hypertensive rats and Wistar-Kyoto rats. *Acta Physiol Scand* 126: 333–339, 1986.
11. **Holstein-Rathlou NH, Marsh DJ.** Oscillations of tubular pressure, flow, and distal chloride concentration in rats. *Am J Physiol Renal Fluid Electrolyte Physiol* 256: F1007–F1014, 1989.
12. **Holstein-Rathlou NH, Marsh DJ.** A dynamic model of the tubuloglomerular feedback mechanism. *Am J Physiol Renal Fluid Electrolyte Physiol* 258: F1448–F1459, 1990.
13. **Holstein-Rathlou NH, Yip KP, Sosnovtseva OV, Mosekilde E.** Synchronization phenomena in nephron-nephron interaction. *Chaos* 11: 417–426, 2001.
14. **Just A, Arendshorst WJ.** Nitric oxide blunts myogenic autoregulation in rat renal but not skeletal muscle circulation via tubuloglomerular feedback. *J Physiol* 569: 959–974, 2005.
15. **Just A, Ehmke H, Wittmann U, Kirchheim HR.** Tonic and phasic influences of nitric oxide on renal blood flow autoregulation in conscious dogs. *Am J Physiol Renal Physiol* 276: F442–F449, 1999.

16. **Kallskog O, Marsh DJ.** TGF-initiated vascular interactions between adjacent nephrons in the rat kidney. *Am J Physiol Renal Fluid Electrolyte Physiol* 259: F60–F64, 1990.

17. **Kriz W, Bankir L.** A standard nomenclature for structures of the kidney. The Renal Commission of the International Union of Physiological Sciences (IUPS). *Kidney Int* 33: 1–7, 1988.

18. **Lachaux JP, Rodriquez E, Le Van Quyen M, Lutz A, Martinerie J, Varela FJ.** Studying single-trials of phase synchronous activity in the brain. *Int J Bifurcat Chaos* 10: 2429–2439, 2000.

19. **Layton AT, Moore LC, Layton HE.** Multistability in tubuloglomerular feedback and spectral complexity in spontaneously hypertensive rats. *Am J Physiol Renal Physiol* 291: F79–F97, 2006.

20. **Layton HE, Pitman EB, Moore LC.** Limit-cycle oscillations and tubuloglomerular feedback regulation of distal sodium delivery. *Am J Physiol Renal Physiol* 278: F287–F301, 2000.

21. **Leyssac PP, Baumbach L.** An oscillating intratubular pressure response to alterations in Henle loop flow in the rat kidney. *Acta Physiol Scand* 117: 415–419, 1983.

22. **Leyssac PP, Holstein-Rathlou NH.** Effects of various transport inhibitors on oscillating TGF pressure responses in the rat. *Pflügers Arch* 407: 285–291, 1986.

23. **Leyssac PP, Holstein-Rathlou NH.** Tubulo-glomerular feedback response: enhancement in adult spontaneously hypertensive rats and effects of anaesthetics. *Pflügers Arch* 413: 267–272, 1989.

24. **Maistrenko YL, Maistrenko VL, Popovych O, Mosekilde E.** Desynchronization of chaos in coupled logistic maps. *Phys Rev E Stat Phys Plasmas Fluids Relat Interdiscip Topics* 60: 2817–2830, 1999.

25. **Malakhov AN.** *Fluctuations in Self-Oscillatory Systems.* Moscow: Nauka, 1968.

26. **Mallat S.** *A Wavelet Guide to Signal Processing.* San Diego, CA: Academic, 1995.

27. **Marsh DJ, Martin CM.** Effects of diuretic states on collecting duct fluid flow resistance in the hamster kidney. *Am J Physiol* 229: 13–17, 1975.

28. **Marsh DJ, Osborn JL, Cowley AW Jr.** 1/f fluctuations in arterial pressure and regulation of renal blood flow in dogs. *Am J Physiol Renal Fluid Electrolyte Physiol* 258: F1394–F1400, 1990.

29. **Marsh DJ, Sosnovtseva OV, Chon KH, Holstein-Rathlou NH.** Nonlinear interactions in renal blood flow regulation. *Am J Physiol Regul Integr Comp Physiol* 288: R1143–R1159, 2005.

30. **Marsh DJ, Sosnovtseva OV, Mosekilde E, Holstein-Rathlou NH.** Vascular coupling induces synchronization, quasiperiodicity, and chaos in a nephron tree. *Chaos* 17: 015114, 2007.

31. **Marsh DJ, Sosnovtseva OV, Pavlov AN, Yip KP, Holstein-Rathlou NH.** Frequency encoding in renal blood flow regulation. *Am J Physiol Regul Integr Comp Physiol* 288: R1160–R1167, 2005.

32. **Mosekilde E, Maistrenko Y, Postnov D.** *Chaotic Synchronization: Applications to Living Systems.* Singapore: World Scientific, 2002.

33. **Peti-Peterdi J.** Calcium wave of tubuloglomerular feedback. *Am J Physiol Renal Physiol* 291: F473–F480, 2006.

34. **Pikovsky A, Rosenblum M, Kuerths J.** *Synchronization.* Cambridge, UK: Cambridge University Press, 2001.

35. **Quiroga R, Kraskov A, Kreuz T, Grassberger P.** Performance of different synchronization measures in real data: a case study on electroencephalographic signals. *Phys Rev E* 65: 041903(14), 2002.

36. **Raghavan R, Chen X, Yip KP, Marsh DJ, Chon KH.** Interactions between TGF-dependent and myogenic oscillations in tubular pressure and whole kidney blood flow in both SDR and SHR. *Am J Physiol Renal Physiol* 290: F720–F732, 2006.

37. **Rosenblum M, Pikovsky A, Kurths J.** Phase synchronization of chaotic oscillations (Abstract). *Phys Rev Lett* 76: 1804, 1996.

38. **Sakai T, Craig DA, Wexler AS, Marsh DJ.** Fluid waves in renal tubules. *Biophys J* 50: 805–813, 1986.

39. **Sejnowski TJ, Paulsen O.** Network oscillations: emerging computational principles. *J Neurosci* 26: 1673–1676, 2006.

40. **Shi Y, Wang X, Chon KH, Cupples WA.** Tubuloglomerular feedback-dependent modulation of renal myogenic autoregulation by nitric oxide. *Am J Physiol Regul Integr Comp Physiol* 290: R982–R991, 2006.

41. **Sosnovtseva OV, Pavlov AN, Mosekilde E, Holstein-Rathlou NH.** Bimodal oscillations in nephron autoregulation. *Phys Rev E Stat Nonlin Soft Matter Phys* 66: 061909, 2002.

42. **Sosnovtseva OV, Pavlov AN, Mosekilde E, Holstein-Rathlou NH, Marsh DJ.** Double-wavelet approach to study frequency and amplitude modulation in renal autoregulation. *Phys Rev E Stat Nonlin Soft Matter Phys* 70: 031915, 2004.

43. **Sosnovtseva OV, Pavlov AN, Mosekilde E, Holstein-Rathlou NH, Marsh DJ.** Double-wavelet approach to studying the modulation properties of nonstationary multimode dynamics. *Physiol Meas* 26: 351–362, 2005.

44. **Stratonovich RL.** *Topics in Theory of Random Noise.* New York: Gordon and Breach, 1963.

45. **Tass P, Rosenblum MG, Weule J, Kurths J, Pikovsky A, Volkmann J, Schnitzler A, Freund HJ.** Detection of n:m phase locking from noisy data: application to magnetoencephalography. *Phys Rev Lett* 81: 3291–3294, 1998.

46. **van Milligen BP, Hidalgo C, Sanchez E.** Nonlinear phenomena and intermittency in plasma turbulence. *Phys Rev Lett* 74: 395–398, 1995.

47. **van Milligen BP, Sanchez E, Estrada T, Hildago C, Branas B, Garcia L.** Wavelet bicoherence: a new turbulence analysis tool. *Phys Plasmas* 2: 3017–3032, 1995.

48. **Wagner AJ, Holstein-Rathlou NH, Marsh DJ.** Internephron coupling by conducted vasomotor responses in normotensive and spontaneously hypertensive rats. *Am J Physiol Renal Physiol* 272: F372–F379, 1997.

49. **Walker M III, Harrison-Bernard LM, Cook AK, Navar LG.** Dynamic interaction between myogenic and TGF mechanisms in afferent arteriolar blood flow autoregulation. *Am J Physiol Renal Physiol* 279: F858–F865, 2000.

50. **Wang H, Kin S, Ju K, Chon KH.** A high resolution approach to estimating time-frequency spectra and their amplitudes. *Ann Biomed Eng* 34: 326–338, 2006.

51. **Wang X, Cupples WA.** Interaction between nitric oxide and renal myogenic autoregulation in normotensive and hypertensive rats. *Can J Physiol Pharmacol* 79: 238–245, 2001.

52. **Yip KP, Holstein-Rathlou NH, Marsh DJ.** Dynamics of TGF-initiated nephron-nephron interactions in normotensive rats and SHR. *Am J Physiol Renal Fluid Electrolyte Physiol* 262: F980–F988, 1992.

53. **Yip KP, Holstein-Rathlou NH, Marsh DJ.** Mechanisms of temporal variation in single-nephron blood flow in rats. *Am J Physiol Renal Fluid Electrolyte Physiol* 264: F427–F434, 1993.

54. **Yip KP, Holstein-Rathlou NH, Marsh DJ.** Chaos in blood flow control in genetic and renovascular hypertensive rats. *Am J Physiol Renal Fluid Electrolyte Physiol* 261: F400–F408, 1991.

55. **Yip KP, Marsh DJ, Holstein-Rathlou NH.** Low dimensional chaos in renal blood flow control in genetic and experimental hypertension. *Physica D* 80: 95–104, 1995.